Journal of Peptide Science
J. Pept. Sci. 2007; **13**: 662–671
Published online 5 September 2007 in Wiley InterScience (www.interscience.wiley.com). DOI: 10.1002/psc.899

JOURNAL OF PEPTIDE SCIENCE

Synthesis and antitumor activity of peptide-paclitaxel conjugates

SERAFIM PAPAS,[a‡] TONIA AKOUMIANAKI,[b‡] CHRISTOS KALOGIROS,[a] LAZAROS HADJIARAPOGLOU,[a] PANAYIOTIS A. THEODOROPOULOS[b] and VASSILIOS TSIKARIS[a]*

[a] Department of Chemistry, University of Ioannina, GR-45110 Ioannina, Greece
[b] Department of Basic Sciences, School of Medicine, University of Crete, 71003 Heraklion, Greece

Received 23 March 2007; Revised 13 April 2007; Accepted 13 April 2007

Abstract: Paclitaxel (Pac) is the most important anticancer drug used mainly in treatment of breast, lung, and ovarian cancer and is being investigated for use as a single agent for treatment of lung cancer, advanced head and neck cancers, and adenocarcinomas of the upper gastrointestinal tract. In this work, we present the synthesis of five 2′-paclitaxel-substituted analogs in which paclitaxel was covalently bound to peptides or as multiple copies to synthetic carriers. Ac-Cys(CH_2CO-2′-Pac)-Arg-Gly-Asp-Arg-NH_2, Folyl-Cys(CH_2CO-2′-Pac)-Arg-Gly-Asp-Ser-NH_2, Ac-[Lys-Aib-Cys(CH_2CO-2′-Pac)]$_2$-NH_2, Ac-[Lys-Aib-Cys(CH_2CO-2′-Pac)]$_3$-NH_2 and Ac-[Lys-Aib-Cys(CH_2CO-2′-Pac)]$_4$-NH_2 were synthesized using 2′-halogeno-acetylated paclitaxel derivatives. Paclitaxel conjugates showed greater solubility in water than paclitaxel and inhibited the proliferation of human breast, prostate, and cervical cancer cell lines. Although all synthesized compounds had an antiproliferative activity, the Ac-[Lys-Aib-Cys(CH_2CO-2′-Pac)]$_4$-NH_2 derivative showed improved biological activity in comparison with paclitaxel in cervical and prostate human cancer cells. Copyright © 2007 European Peptide Society and John Wiley & Sons, Ltd.

Keywords: artificial carriers; paclitaxel antitumor agents; paclitaxel derivatives; paclitaxel ESI-MS; taxol derivatives; thioether bond

INTRODUCTION

Paclitaxel (taxol) (Figure 1), the most important anticancer drug isolated from the bark of the Pacific Yew tree *Taxus brevifolia* [1], is widely used in the treatment of human carcinomas especially breast, lung, and ovarian cancer [2]. Its anticancer activity stems from the ability of promoting microtubule assembly and stabilization, cell cycle arrest at the G2/M phase of the cell cycle, organizational and functional alteration of the nuclear envelope, and cell death [3,4]. A major problem for the clinical use of this drug is the low solubility in water (<4 μg/ml) [5] and in most pharmaceutically acceptable solvents [6]. It is usually administrated in a vehicle containing Cremophor EL (polyethoxylated castor oil), which has been demonstrated to cause important clinical side effects, such as severe anaphylactoid hypersensitivity reactions, hyperlipidemia, abnormal lipoprotein patterns, aggregation of erythrocytes, and peripheral neuropathy [7]. A great amount of research effort has been paid aiming either to establish a synthetic root for the total and semisynthesis of paclitaxel [8–13] or to develop paclitaxel derivates with improved water solubility, antitumor activity, and facile cellular uptake [14–16]. From structure–activity relationships studies, it has been concluded that both the 2′ and 7 hydroxyl groups in paclitaxel are suitable for linking ester derivatives [17]. Although modifications at the 2′-position of paclitaxel resulted in loss of the activity to promote tubulin polymerization, such modified compounds retained cytotoxicity or the *in vivo* antitumor activity [15]. Furthermore, esters at the 2′-position are labile and therefore provide the possibility of developing 'inactive' prodrugs, which could be unmasked *in vivo* to release active paclitaxel. From the chemical point of view, the hydroxyl group at the 2′-position of paclitaxel is more reactive than the sterically hindered 7-hydroxyl group. Thus, paclitaxel derivatives at 2′-position are usually synthesized without protection of the other functional groups [18]. These observations led to the synthesis of a large number of paclitaxel prodrugs. Water soluble and high half-life conjugates have been produced by coupling paclitaxel at 2′-position with molecular transporters, such as folic acid and arginine-rich peptides [19–22].

In this work, we present the synthesis of analogs in which paclitaxel was covalently bound to peptides or as multiple copies to synthetic carriers aiming at either the improvement of the water solubility and/or cytotoxic activity of paclitaxel. For the covalent attachment of paclitaxel we used the Ac-Cys-Arg-Gly-Asp-Arg-NH_2 and Folyl-Cys-Arg-Gly-Asp-Ser-NH_2 peptides and a new oligopeptide carrier. Both -Arg-Gly-Asp- sequence and folic acid were selected as marking moieties of integrin and folate receptors, which are tumor overexpressed and can be differentially targeted [23]. The carrier, formed by the repetitive sequence -Lys-Aib-Cys- was designed to contribute both to solubility and the

*Correspondence to: Vassilios Tsikaris, Department of Chemistry, University of Ioannina, GR-45110 Ioannina, Greece;
e-mail: btsikari@cc.uoi.gr
‡ Equal contribution.

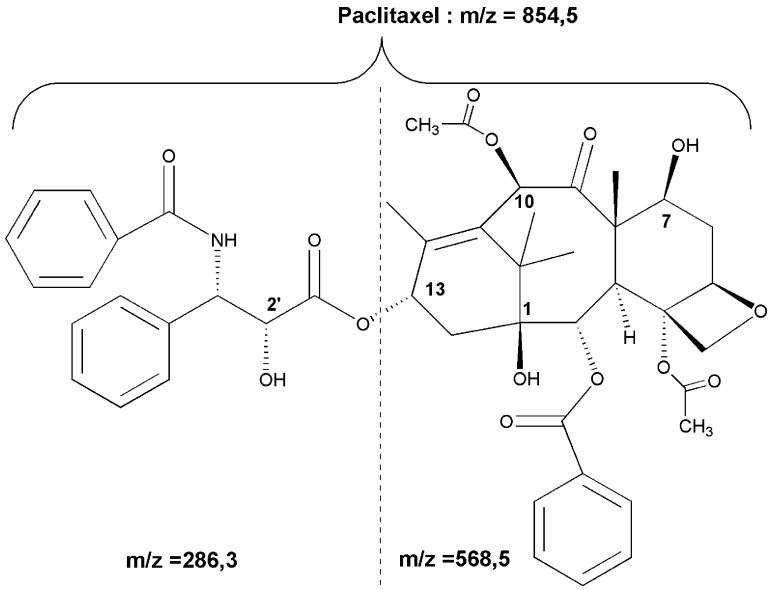

Figure 1 The structure of paclitaxel. Dotted line shows the position of fragmentation in the ESI-MS spectra.

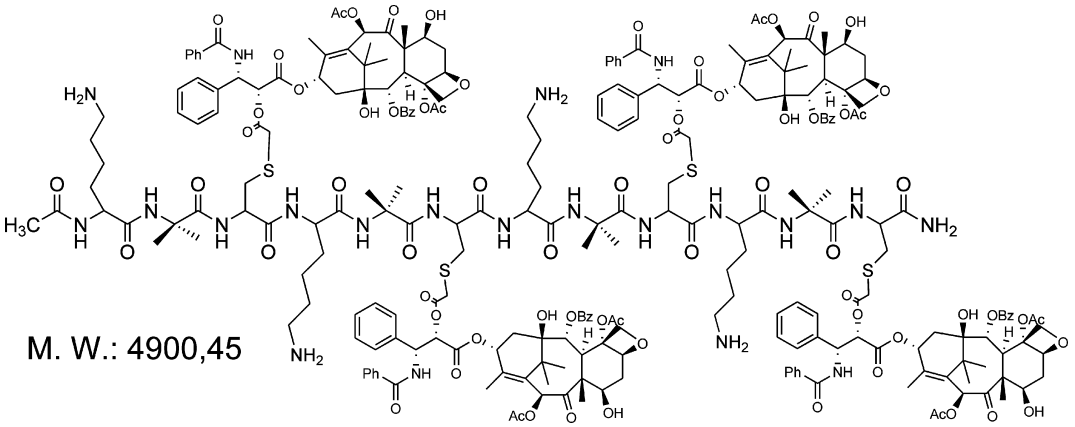

Figure 2 Schematic representation of Ac-[Lys-Aib-Cys(CH_2CO-2′-Pac)]$_4$-NH_2.

specific chemistry needed for paclitaxel conjugation because it allows the covalent attachment of a properly modified paclitaxel in multiple copies linked by a thioether bond (Figure 2). The Lys side-chain amino group could contribute to a greater solubility of the conjugate in water, while Aib was chosen to induce helical properties to the carrier [24–27]. This latter could avoid intramolecular interactions between the conjugated paclitaxel molecules, thereby facilitating their binding to tubulin. We found that the synthesized peptide-paclitaxel derivatives possess higher solubility in water than paclitaxel and inhibit the proliferation of human breast, prostate, and cervical cancer cell lines.

MATERIALS AND METHODS

Reagents

Abbreviations used in this paper follow the guidelines by Jones [28]. Paclitaxel was purchased from Sigma (Deisenhofen, Germany). Fmoc amino acid derivatives, HBTU, and HOBt were purchased from Neosystem Laboratoire, (Strasbourg, France). 4-(2′,4′-Dimethoxyphenyl-Fmoc-aminomethyl)-phenoxymethyl-linked polystyrene (Rink amide) and 4-(hydroxymethyl) phenoxymethyl-linked polystyrene (Wang) resins were obtained from GL Biochem (Shanghai, China). Triisopropylsilane (TIS), 1,2 ethane dithiol (EDT), DIEA, TFA, dimethoxybenzene (DMB), piperidine, chloroacetic anhydride, iodoacetic anhydrite, and bromoacetyl bromide were Merck-Schuchardt (Darmstadt, Germany) products and used without further purification. DCM, DMF distilled over ninhydrin and stored under preactivated molecular sieves of 4 Å, and the gradient degree HPLC solvents acetonitrile and methanol were purchased from Labscan, (Dublin, Ireland).

HPLC Analysis

The analytical HPLC chromatograms were run on a Waters Millenium (Milford, USA) apparatus with a photodiode array detector 996. The spectra were acquired at 214 and 280 nm. A reverse-phase Discovery C18 column and a flow rate of

DOI: 10.1002/psc

1 ml/min were used. The crude peptides and the paclitaxel derivatives or conjugates were purified by semipreparative HPLC on a Water PrepLC 4000 system associated with a reversed-phase Discovery C18 column (25 cm × 10 mm) running at a flow rate of 4.7 ml/min.

Electrospray Ionization Mass Spectroscopy

Electrospray ionization mass spectra (ESI-MS) were recorded on a Micromass (Manchester, England) Platform II quadrupole mass spectrometer. Samples were dissolved in a mixture of H_2O (0.1%TFA)/CH_3CN (0.1%TFA) (1/1, v/v) and injected into the ESI source at a flow rate of 5 µl/min. The source temperature was adjusted at 70 °C, while the cone voltage was set at the desired value (30–140 V).

Peptide Synthesis

The Ac-Cys-Arg-Gly-Asp-Arg-NH_2, Folyl-Cys-Arg-Gly-Asp-Ser-NH_2, and Ac-[Lys-Aib-Cys]$_n$-NH_2, $n = 2$–4, peptides used for paclitaxel conjugation were synthesized on a Rink amide resin by the solid-phase peptide synthesis methodology using the Fmoc/Bu^t strategy [29]. Amino acids were introduced protected as Fmoc-Lys(Mtt)-OH, Fmoc-Cys(Trt)-OH, Fmoc-Aib-OH, Fmoc-Asp(Bu^t)-OH, Fmoc-Ser(Bu^t)-OH and Fmoc-Arg(Pbf)-OH. The folic acid was incorporated without protection of either α- or γ-carboxylic group. Fmoc deprotection steps were carried out with 20% piperidine in DMF (v/v) for 15 min. Coupling reactions of Fmoc amino acids were performed in DMF using a molar ratio of amino acid/HBTU/HOBt/DIEA/resin (3 : 3 : 3 : 6 : 1). Reactions were monitored with the color Kaiser test. The amino terminus end was acetylated using 30-fold excess of acetic anhydride in pyridine. The simultaneous deprotection and cleavage of the peptides from the resin was done by applying Reagent I (92.5% TFA/2.5% TIS/5% DMB) [30]. After 3 h of stirring, the resin was filtered and washed with TFA. The combined filtrates were concentrated under reduced pressure. Hexane was added and the mixture was reconcentrated. This procedure was performed twice. The peptides were precipitated with cold diethyl ether, filtered, dissolved in 2N acetic acid, and lyophilized. The data of the synthesized peptides are summarized in Table 1.

2′-Bromoacetyl-Paclitaxel

Paclitaxel (0.022 mmol, 18.8 mg) was dissolved in 2 ml DCM under nitrogen atmosphere in dark. The solution was cooled to 0 °C in an ice bath and 0.03 mmol (2.6 µl) bromoacetyl bromide and 0.06 mmol (10.3 µl) DIEA were added consecutively. The reaction was monitored by ESI-MS and stopped after 1 h. The reaction mixture was diluted with DCM, the organic mixture was washed successively two times with 0.1 N HCl, water, saturated solution of $NaHCO_3$, and water, and dried with Na_2SO_4. After evaporation of the solvent, the solid residue was dissolved in H_2O (0.1% TFA)/CH_3CN (0.1% TFA), (1 : 1, v/v) and subjected to purification by semipreparative HPLC. Gradient elution was performed with the following solvents: A, H_2O/0.1%TFA and B, CH_3CN/0.1% TFA from 60 to 5% A for 30 min ($R_t = 16.5$ min). The overall yield was 78%. Expected MW = 974.84. Found MW = 974.65 ($[M + H]^+ = 975.65$). The bromoacetylated group of paclitaxel was confirmed by recording the ESI-MS spectra at various cone voltages. By increasing the applied cone voltage, fragmentation occurs at the position shown in Figure 1.

2′-Chloroacetyl-Paclitaxel

Paclitaxel (0.014 mmol, 12 mg) was dissolved in 2 ml DCM under nitrogen atmosphere in dark. The solution was cooled to 0 °C in an ice bath, and 0.017 mmol (2.9 mg) chloroacetic anhydride and 0.017 mmol (2.9 µl) DIEA were added consecutively [20]. The reaction was monitored by ESI-MS and stopped after 3 h. The reaction mixture was washed two times with 0.1 N HCl, water, and a saturated solution of $NaHCO_3$ and dried with Na_2SO_4. After evaporation of the solvent, the solid residue was dissolved in H_2O (0.1% TFA)/CH_3CN (0.1% TFA) (1 : 1, v/v) and injected to semipreparative HPLC. The elution system A, H_2O/0.1% TFA and B, CH_3CN/0.1% TFA from 90 to 5% A for 30 min was used for the purification ($R_t = 24$ min). The overall yield was 70%.

Table 1 ESI-MS and HPLC data of the synthesized compounds

Compound	Expected MW	Found MW	Retention[a] time (min)
2′-Chloroacetyl-paclitaxel	930.43	930.21	24
2′-Bromoacetyl-paclitaxel	974.84	974.65	16.5
2′-Iodoacetyl-paclitaxel	1021.84	1021.85	12
Ac-Cys-Arg-Gly-Asp-Arg-NH_2	646.72	646.67	7.4
Folyl-Cys-Arg-Gly-Asp-Ser-NH_2	958.96	959.19	11
Ac-[Lys-Aib-Cys]$_2$-NH_2	691.91	691.74	—
Ac-[Lys-Aib-Cys]$_3$-NH_2	1008.33	1008.18	—
Ac-[Lys-Aib-Cys]$_4$-NH_2	1324.75	1324.73	—
Ac-Cys(CH_2CO-2′-Pac)-Arg-Gly-Asp-Arg-NH_2	1540.70	1540.82	17
Folyl-Cys(CH_2CO-2′-Pac)-Arg-Gly-Asp-Ser-NH_2	1852.88	1853.50	15
Ac-[Lys-Aib-Cys(CH_2CO-2′-Pac)]$_2$-NH_2	2478.90	2480.68	19
Ac-[Lys-Aib-Cys(CH_2CO-2′-Pac)]$_3$-NH_2	3690.11	3690.57	28
Ac-[Lys-Aib-Cys(CH_2CO-2′-Pac)]$_4$-NH_2	4900.45	4901.50	22

[a] For the gradient elution systems see 'Materials and Methods'.

DOI: 10.1002/psc

Expected MW = 930.43. Found M.W. = 930.21 ($[M + H]^+$ = 931.21).

2′-Iodoacetyl-Paclitaxel

Paclitaxel (0.012 mmol, 10.2 mg) was dissolved in 1.5 ml DCM under argon atmosphere in dark. The solution was cooled to 0 °C in an ice bath, and 0.02 mmol (7 mg) iodoacetic anhydride and 0.02 mmol (3.4 μl) DIEA were added consecutively. The reaction was monitored by ESI-MS and stopped after 3 h. The reaction mixture was diluted with DCM, washed successively two times with 0.1 N HCl, water, a saturated solution of $NaHCO_3$, and water and dried with Na_2SO_4. After evaporation of the solvent, the solid residue was dissolved in H_2O (0.1% TFA)/CH_3CN·(0.1% TFA), (1 : 1, v/v) and subjected to purification by semipreparative HPLC. Gradient elution was performed with the following solvents: A, H_2O/0.1% TFA and B, CH_3CN/0.1% TFA from 50 to 5% A for 30 min (R_t = 12 min). The overall yield was 75%. Expected MW = 1021.84. Found MW = 1021.85 ($[M + H]^+$ = 1022.85).

Ac-Cys(CH_2CO-2′-Pac)-Arg-Gly-Asp-Arg-NH_2

2′-Chloroacetyl-paclitaxel (0.012 mmol, 11.2 mg) was dissolved in 0.5 ml DMF at room temperature under argon atmosphere in dark and 0.013 mmol DIEA (2.2 μl) was added. To the resulting solution, 0.0117 mmol (10.2 mg) Ac-Cys-Arg-Gly-Asp-Arg-NH_2·2TFA was added in small portions. After 3.5 h, the reaction was completed as revealed by ESI-MS. H_2O (0.1% TFA)/CH_3CN (·0.1% TFA) was added to the reaction mixture and the resulting solution was subjected to HPLC purification without any further manipulation. Gradient elution was performed with the following solvents: A, H_2O/0.1% TFA and B, CH_3CN/0.1% TFA from 90 to 5% A for 30 min (R_t = 17 min). The desired product was isolated at an overall yield of 38%. Expected MW = 1540.70. Found MW = 1540.82 ($[M + 2H]^{2+}/2$ = 771.41). The recorded ESI-MS spectra at 40, 60, and 80 V cone voltages (Figure 3) suggest that the most sensitive bond of the conjugate is the C13 C–O bond of paclitaxel which links baccatin with the side-chain.

Folyl-Cys(CH_2CO-2′-Pac)-Arg-Gly-Asp-Ser-NH_2

2′-Bromoacetyl paclitaxel (0.0031 mmol, 3 mg) was dissolved in 1.4 ml of a mixture of CH_3CN/H_2O/DMF (2/1/1, v/v/v) under argon atmosphere in dark. The solution was cooled to 0 °C in an ice bath and 0.003 mmol (0.53 μl) DIEA was added. To this cooled solution, 0.0028 mmol (3.0 mg) Folyl-Cys-Arg-Gly-Asp-Ser-NH_2·TFA was added in small portions. The reaction was monitored by ESI-MS and after 5 h the reaction was stopped by the addition of 4 ml of H_2O·(0.1% TFA)/CH_3CN (0.1% TFA) to the reaction mixture. The resulting solution was subjected to HPLC purification, without any further manipulation, using as gradient elution system A (H_2O/0.1%TFA) and B (CH_3CN/0.1% TFA) from 80 to 5% A for 40 min (R_t = 15 min). The desired product was isolated at an overall yield of 12%. Expected MW = 1852.88. Found MW = 1853.50 ($[M + 2H]^{2+}/2$ = 927.75).

Ac-(Lys-Aib-Cys(CH_2CO-2′-Pac))$_2$-NH_2

2′-Chlorooacetyl paclitaxel (0.0121 mmol, 11.3 mg) was dissolved in 1.5 ml of a mixture of CH_3CN/H_2O (2/1, v/v) under N_2 atmosphere. Following the addition of 0.023 mmol (4 μl) DIEA, 0.0041 mmol (3.8 mg) of Ac-(Lys-Aib-Cys)$_2$-NH_2·2TFA was added in small portions. The reaction was monitored by ESI-MS, and after 6 h the reaction was stopped by the addition of 4 ml of H_2O (0.1% TFA)/CH_3CN (0.1% TFA). The resulting mixture, without any other manipulation, was subjected to HPLC purification using as gradient elution system A (H_2O/0.1% TFA) and B (CH_3CN/0.1% TFA) from 70 to 30% A for 40 min (R_t = 19 min). The desired product was isolated at an overall yield of 40%. Expected MW = 2478.90. Found MW = 2480.68 ($[M + 2H]^{2+}/2$ = 1241.34).

Ac-(Lys-Aib-Cys(CH_2CO-2′-Pac))$_3$-NH_2

2′-Bromoacetyl paclitaxel (0.0118 mmol, 11.5 mg) was dissolved in 1.5 ml of a mixture of CH_3CN/H_2O (2/1, v/v) under N_2 atmosphere and 0.0234 mmol (4 μl) DIEA was added. The solution was cooled to 0 °C in an ice bath and 0.0033 mmol (4.5 mg) of Ac-(Lys-Aib-Cys)$_3$-NH_2·3TFA was added in small portions. The reaction was monitored by ESI-MS. After 6 h, the reaction was stopped by the addition of 4 ml of H_2O (0.1% TFA)/CH_3CN (0.1% TFA). The resulting mixture, without any other manipulation, was subjected to HPLC purification using as gradient elution system A (H_2O/0.1% TFA) and B (CH_3CN/0.1% TFA) from 90 to 5% A for 40 min (R_t = 28 min). The overall yield was 32%. Expected MW = 3690.11. Found MW = 3690.57 ($[M + 3H]^{3+}/3$ = 1231.17).

Ac-(Lys-Aib-Cys(CH_2CO-2′-Pac))$_4$-NH_2

2′-Bromoacetyl-paclitaxel (0.015 mmol, 14.6 mg) was dissolved in 2 ml of a mixture of CH_3CN/H_2O (2/1, v/v) under N_2 atmosphere and 0.029 mmol (5 μl) DIEA was added. The solution was cooled to 0 °C in an ice bath and 0.0025 mmol (4.4 mg) of Ac-(Lys-Aib-Cys)$_4$-NH_2·4TFA was added in small portions. The reaction was monitored by ESI-MS. After 6 h, the reaction was stopped by the addition of 3 ml of H_2O (0.1% TFA)/CH_3CN (0.1% TFA). The resulting mixture, without any other manipulation, was subjected to HPLC purification using as gradient elution system A [H_2O (0.1% TFA)/CH_3CN (0.1% TFA) (70/30, v/v)] and B [H_2O (0.1% TFA)/CH_3CN (0.1% TFA), (5/95, v/v)] from 100 to 0% A for 40 min (R_t = 22 min). The overall yield of the desired conjugate (Figure 3) was 27%. Expected MW = 4900.45. Found MW = 4901.50 ($[M + 3H]^{3+}/3$ = 1635.56, $[M + 4H]^{4+}/4$ = 1225.97).

Biological Assays

Cell lines and culture. Cell lines from mammary (MCF-7), cervical (HeLa), and prostate (DU) adenocarcinoma obtained from American Type Tissue Culture Collection (Manassas, VA) were maintained at 37 °C in a humidified atmosphere containing 5% CO_2. MCF-7 cells were cultured in DMEM/HAM'S F-12 plus 10 μg/ml insulin; HeLa and DU cells in Dulbecco's MEM. All media were purchased from Biochrom (Berlin, Germany) and were supplemented with 10% heat-inactivated fetal bovine serum, penicillin, and streptomycin.

Cell treatments. Upon reaching 50–60% confluence, cells grown either on culture dishes or on coverslips were incubated with paclitaxel (Taxol, Bristol-Meyer Squibb, N. Jersey, USA) or paclitaxel analogs diluted in culture medium at the

DOI: 10.1002/psc

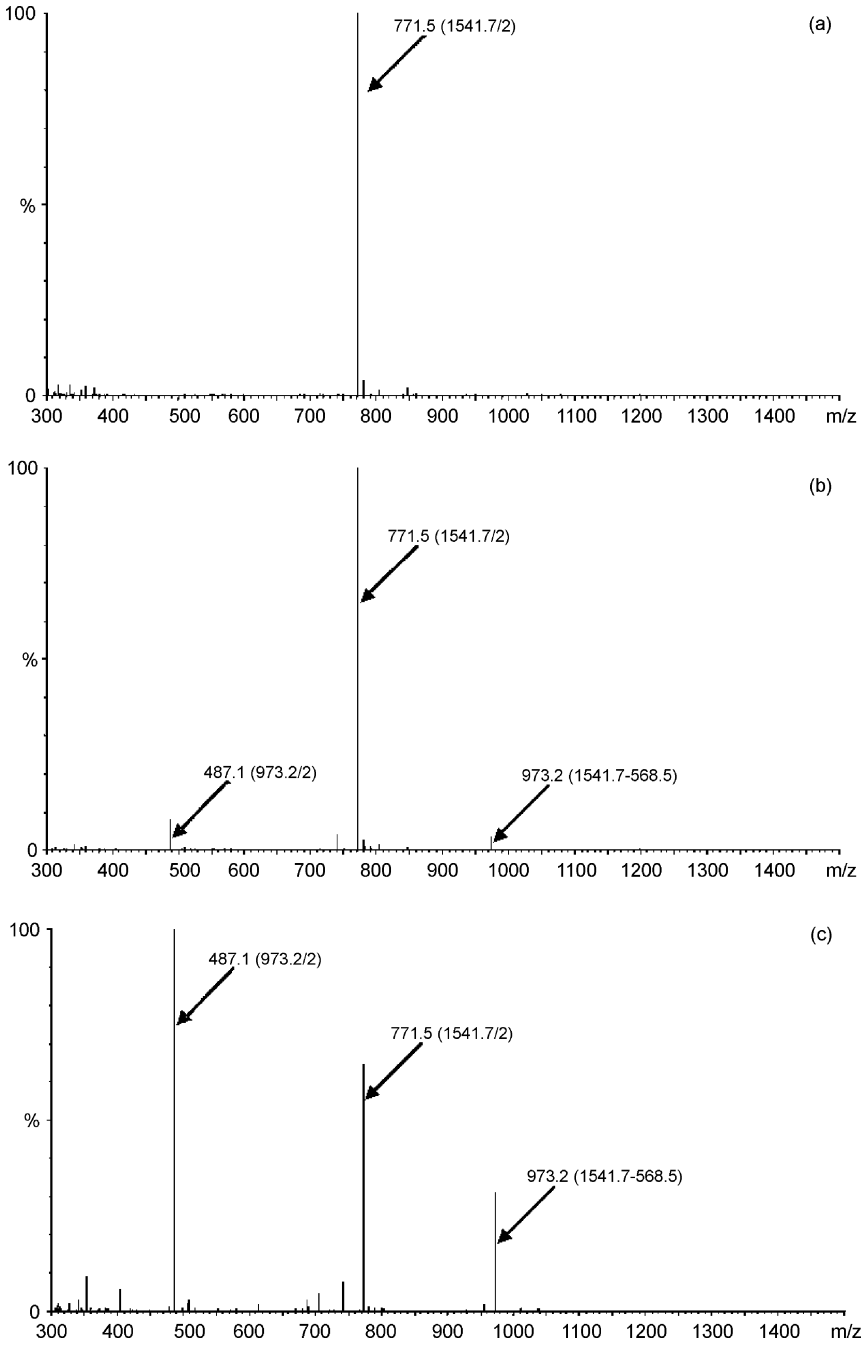

Figure 3 ESI-MS spectra of Ac-C(CH_2CO-2′-Pac)RGDR-NH_2 recorded with cone voltage 40 V (a), 60 V (b) and 80 V (c). The fragmentation occurs at the C13 C–O bond (−568.5 Da) of paclitaxel which links baccatin with the side-chain.

concentrations indicated, at 37 °C for 24 h, washed with fresh medium, and incubated in a drug-free medium at 37 °C for up to 3 days.

Cell proliferation assay. Cells were grown on 24-well plates, and after the various treatments cell proliferation was determined using MTT (3-[4,5-dimethylthiazol-2-yl]-2,5-diphenyltetrazolium bromide; Thiazol blue), as specified by the supplier (Sigma Chemical Co, St Louis, MO). The percentages of viable cells for each treatment were determined by measurement of MTT absorbance, relative to the initial cell population before any treatment. All cell proliferation data are means of eight measurements from three independent experiments.

Cell cycle analysis. Adherent cells were trypsinized, washed with PBS, and treated in order to stain the DNA using the DNA-Prep Coulter Reagent Kit (Beckman Coulter), as specified by the supplier. Samples were subjected to fluorescence-activated cell sorter (FACS) in a Coulter Epics Elite.

Examination of nuclear morphology and nuclear envelope integrity by indirect immunofluorescence microscopy. Indirect immunofluorescence was performed as described previously [4]. Briefly, cells grown on coverslips were washed

DOI: 10.1002/psc

with PBS, fixed in 4% formaldehyde for 5 min at room temperature, and permeabilized with Triton X-100. The antibodies used included an anti-β-tubulin monoclonal (clone TUB 2.1) obtained from Sigma Chemical Co (St Louis, MO) and an antilamin B polyclonal [4]. Chromatin was stained with the DNA-binding dye, Topro, and specimens were visualized in a Leica SP confocal microscope. The morphology of interphase nuclei and the integrity of the nuclear envelope were assessed after examination of at least 500 nuclei per sample.

RESULTS AND DISCUSSION

The synthesis of paclitaxel conjugates was performed by employing 2′-functionalized chloro, bromo, or iodo-acetylated paclitaxel derivatives. All the halogeno-acetylated paclitaxel derivatives were obtained in high yields by using as starting material unprotected paclitaxel. The ESI-MS technique was shown to be a valuable and facile method to reveal the progress of the esterification reaction. By increasing the applied cone voltage, fragmentation occurs at 2′-functionalized chloro, bromo, or iodo-acetylated paclitaxel derivatives liberating the side-chain of paclitaxel [31]. The same phenomenon occurred at the Ac-Cys(CH_2CO-2′-Pac)-Arg-Gly-Asp-Arg-NH_2 and Folyl-Cys(CH_2CO-2′-Pac)-Arg-Gly-Asp-Ser-NH_2 paclitaxel conjugates (Figure 3), while higher cone voltages were necessary (>120 V) in the case of Ac-[Lys-Aib-Cys(CH_2CO-2′-Pac)]$_n$-NH_2, $n = 2$–4. This result, combined with the fact that no paclitaxel was released under these experimental conditions (Figure 3), indicates an increased stability to cleavage of the 2′-ester bond.

The formation of the thioether bond was effective with both the 2′-bromo- and chloroacetyl paclitaxel, although conjugation of the sequential oligopeptide carrier with 2′-bromoacetyl paclitaxel was more efficient than that observed with the chloro derivative. For example, reaction of Ac-[Lys-Aib-Cys]$_4$-NH_2 with chloroacetyl paclitaxel failed to yield the desired compound, whereas conjugation of chloroacetyl paclitaxel with other oligopeptide carriers resulted in a high percentage of dimer owing to the long reaction times needed. In contrast, during the reaction of conjugation using bromoacetylated paclitaxel the dimerization of the Cys-containing component was minimized, probably because of the high reactivity of the bromo- derivative. Conjugation of paclitaxel to -Arg-Gly-Asp-containing peptides or to the sequential oligopeptide carrier Ac-[Lys-Aib-Cys]$_n$-NH_2, $n = 2,3$ provided derivatives soluble in water. However, the solubility was greatly reduced in the case of Ac-[Lys-Aib-Cys(CH_2CO-2′-Pac)]$_4$-NH_2.

Biological activity of the synthesized analogs was first evaluated by determining their capacity to inhibit proliferation of human epithelial cervical (HeLa), breast (MCF-7), and prostate (DU) cancer cells. Equal concentrations of paclitaxel and Ac-[Lys-Aib-Cys(CH_2CO-2′-Pac)]$_n$-NH_2 analogs containing two, three, or four molecules of paclitaxel were added to the cell cultures for 24 h, the drugs were then removed, and the cells were cultured for 72 h in a drug-free medium. The percentage of viable cells was determined using MTT assay. The calculated IC_{50} (the concentration which inhibits 50% of cell proliferation) for each of the drugs is presented in Table 2.

All compounds showed IC_{50} in the nanomolar range. However, the analog Ac-[Lys-Aib-Cys(CH_2CO-2′-Pac)]$_4$ -NH_2 (tetra) inhibited the proliferation of cancer cells more efficiently than the other synthetic analogs and paclitaxel itself. It must be noted here that the antiproliferative activity of tetra in HeLa and DU cells was statistically higher than that of paclitaxel, especially when used at very low concentrations (Figure 4). In addition, DU cells were more sensitive to Ac-[Lys-Aib-Cys(CH_2CO-2′-Pac)]$_4$ -NH_2 than HeLa cells. Specifically, Ac-[Lys-Aib-Cys(CH_2CO-2′-Pac)]$_4$-NH_2 was statistically more effective than paclitaxel when used in DU cells at concentrations from 1 to 10 nM, whereas in HeLa cells it was more potent only at 1 and 3 nM. It is of interest to note that in prostate cancer cells Ac-[Lys-Aib-Cys(CH2CO-2′-Pac)]$_4$-NH_2 exerted a net cytotoxic effect (decrease of the number of viable cells below the initial population) in lower concentrations (10 nM) than paclitaxel (20 nM).

To understand the basis of the increased antiproliferative activity of Ac-[Lys-Aib-Cys(CH_2CO-2′-Pac)]$_4$-NH_2, we investigated the effect of both compounds on cell cycle arrest at the G2/M phase and the nuclear morphology and nuclear envelope organization in HeLa and DU cells.

Table 3 shows that tetra was more efficient than paclitaxel in arresting HeLa and DU cells that have been treated for 24 h with 10 nM of either drug. More importantly, this arresting effect persisted in both cell lines when released from Ac-[Lys-Aib-Cys(CH_2CO-2′-Pac)]$_4$-NH_2 and cultured for an additional 24 h in a drug-free medium, while cells released from paclitaxel treatment showed similar percentages of G2/M population as for nontreated (control)

Table 2 IC_{50} of paclitaxel and Ac-[Lys-Aib-Cys(CH_2CO-2′-Pac)]$_n$-NH_2 conjugates with two (dimeric), three (trimeric) or four (tetra) molecules of paclitaxel

	Paclitaxel (nM)	Dimeric (nM)	Trimeric (nM)	Tetra (nM)
Hela	1.29	1.31	1.70	0.96
DU	2.67	2.85	3.88	1.30
MCF-7	0.90	0.62	3.00	0.64

DOI: 10.1002/psc

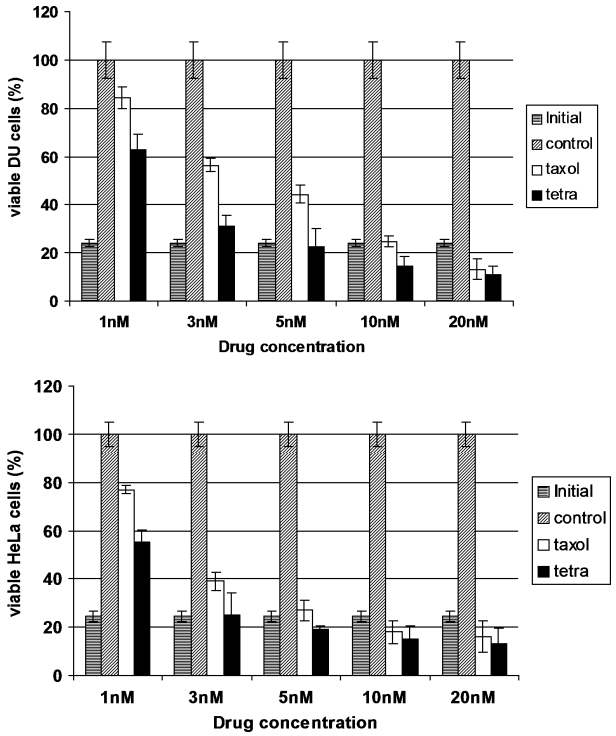

Figure 4 Viability of HeLa and DU cells treated with various concentrations of paclitaxel (taxol) and the analog Ac-[Lys-Aib-Cys(CH_2CO-2′-Pac)]$_4$-NH_2, (tetra) for 24 h and then cultured in a drug-free medium for 72 h. Viable cells were determined using the MTT assay. Results are expressed as percentages of viable cells compared to nontreated cells (control). The starting cell population before any treatment is denoted as 'initial'.

Table 3 Percentage of HeLa and DU Cells in the G2/M phase in untreated cultures (control) or cells treated with paclitaxel or the analog Ac-[Lys-Aib-Cys(CH_2CO-2′-Pac)]$_4$-NH_2, (tetra) for 24 h (24 h) and then cultured in a drug-free medium for more 24 h (24 h + 24 h)

Compound/concentration	Hela		DU	
	24 h	24 h + 24 h	24 h	24 h + 24 h
Paclitaxel/3 nM	11	12	26	23
Paclitaxel/10 nM	41	23	48	26
Tetra/3 nM	19	20	30	32
Tetra/10 nM	52	47	60	54
Control	20	19	26	24

cells. However, we show that incubation of both cell lines with very low concentrations (3 nM), which inhibit cell proliferation (Figure 4), did not induce cell cycle arrest at the G2/M phase of the cell cycle (Table 3). It is known that paclitaxel-treated cells pass through and complete the cell cycle when the intracellular concentration of the drug is insufficient to stabilize microtubules. This is common for paclitaxel-arrested cells at the G2/M phase that are cultured in a drug-free medium, or for cells treated with very low concentrations of paclitaxel [4,32]. Many of these cells have been observed to develop multiple or lubulated nuclei, with abnormally arranged nuclear pores and numerous gaps in the nuclear lamina, whereas the macromolecular trafficking through the nuclear pores of these cells was altered [4,33]. Therefore, we examined the nuclear morphology and nuclear envelope integrity of HeLa and DU cells that were treated with 3 nM of either paclitaxel or Ac-[Lys-Aib-Cys(CH_2CO-2′-Pac)]$_4$-NH_2 and then cultured in a drug-free medium for 72 h. Many HeLa (Figure 5) and DU (Figure 6) cells treated with paclitaxel or Ac-[Lys-Aib-Cys(CH_2CO-2′-Pac)]$_4$-NH_2 had abnormally shaped nuclei that often presented nuclear envelope discontinuity. This phenotype was shown to originate, at least partially, from defects in cell division, namely incorrect cytokinesis and sorting of nuclear envelope components (Figures 5 and 6). To compare the effectiveness of both drugs to produce cells with abnormally shaped nuclei, we examined the nuclear morphology of at least 500 cells for each treatment and cell line (Table 4). We found that treatment with Ac-[Lys-Aib-Cys(CH_2CO-2′-Pac)]$_4$-NH_2 was more effective than paclitaxel in producing cells with multinucleated phenotype in both cell lines.

The sum of our results indicate that the tetra compound exerted an enhanced antiproliferative effect in cancer cell lines compared to paclitaxel, which could be explained by the sustained cell cycle arrest and the increased number of multinucleated cells following treatment with the paclitaxel analog.

CONCLUSIONS

In this study five paclitaxel-peptide conjugates were successfully synthesized combining SPPS and chemoselective ligation methods. The 2′-bromoacetyl paclitaxel has been found to be the most effective

Table 4 Nuclear shape of HeLa and DU cells treated with 3 nM paclitaxel or the analog Ac-[Lys-Aib-Cys(CH_2CO-2′-Pac)]$_4$-NH_2, (tetra) for 24 h and then cultured in a drug-free medium for 72 h. More than 500 cells for each treatment were examined under a fluorescence microscope and the results are expressed as a percentage of cells with normal, lobulated, and multinucleated nuclear phenotype

Drug/cell line	Cells with nuclear shape (%)		
	Normal	Lobulated	Multinucleated
Paclitaxel/Hela	23	63	14
Tetra/Hela	17	53	30
Paclitaxel/DU	14	81	5
Tetra/DU	6	68	26

DOI: 10.1002/psc

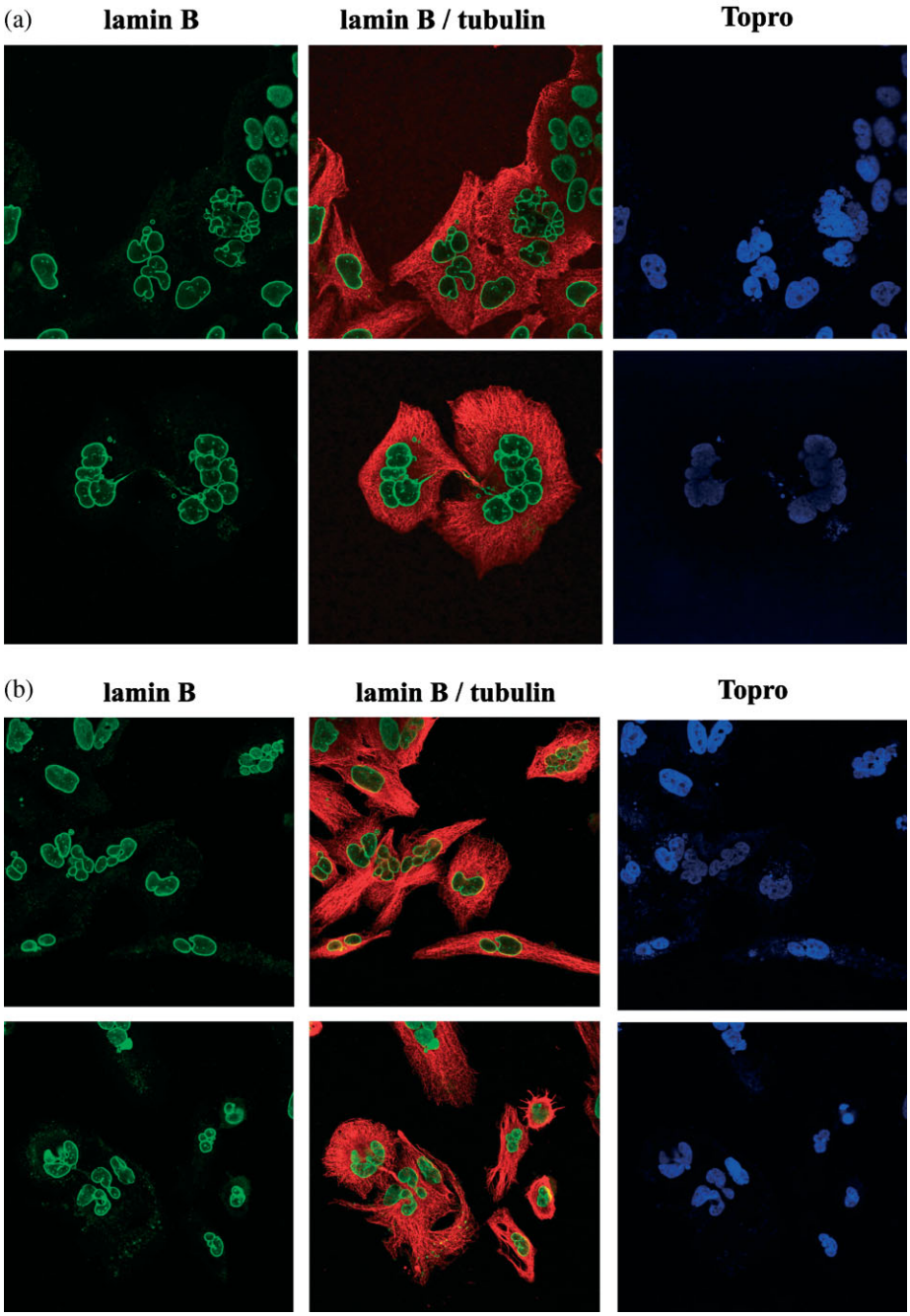

Figure 5 Representative images of HeLa cells treated with paclitaxel (A) and Ac-[Lys-Aib-Cys(CH_2CO-2′-Pac)]$_4$-NH_2 (tetra) (B). Cells that have been incubated with 3 nM of either drug for 24 h were cultured in a drug-free medium for 72 h and then immunostained for nuclear envelope (lamin B, green) microtubules (tubulin, red), and DNA (Topro, blue). Note the lagged or dispersed lamin B during cytokinesis of cells in the lower row of panels A and B.

intermediate for the formation of the thioether bond in Cys-containing sequential oligopeptide carriers. The increased reactivity of this compound probably contributed to avoidance of extended dimerization. The -Arg-Gly-Asp-containing paclitaxel conjugates were very soluble in water. In contrast, the solubility of Ac-[Lys-Aib-Cys(CH_2CO-2′-Pac)]$_n$-NH_2, conjugates decreased as the number of conjugated paclitaxel copies increased. Although all the synthesized compounds had an antiproliferative activity, the Ac-[Lys-Aib-Cys(CH_2CO-2′-Pac)]$_4$-NH_2 derivative showed improved biological activity in comparison with paclitaxel in cervical and prostate human cancer cells.

Acknowledgements

This work was financially supported by the EU and the Greek General Secretariat for Research and Technology (No. PENED 01ÅÄ376).

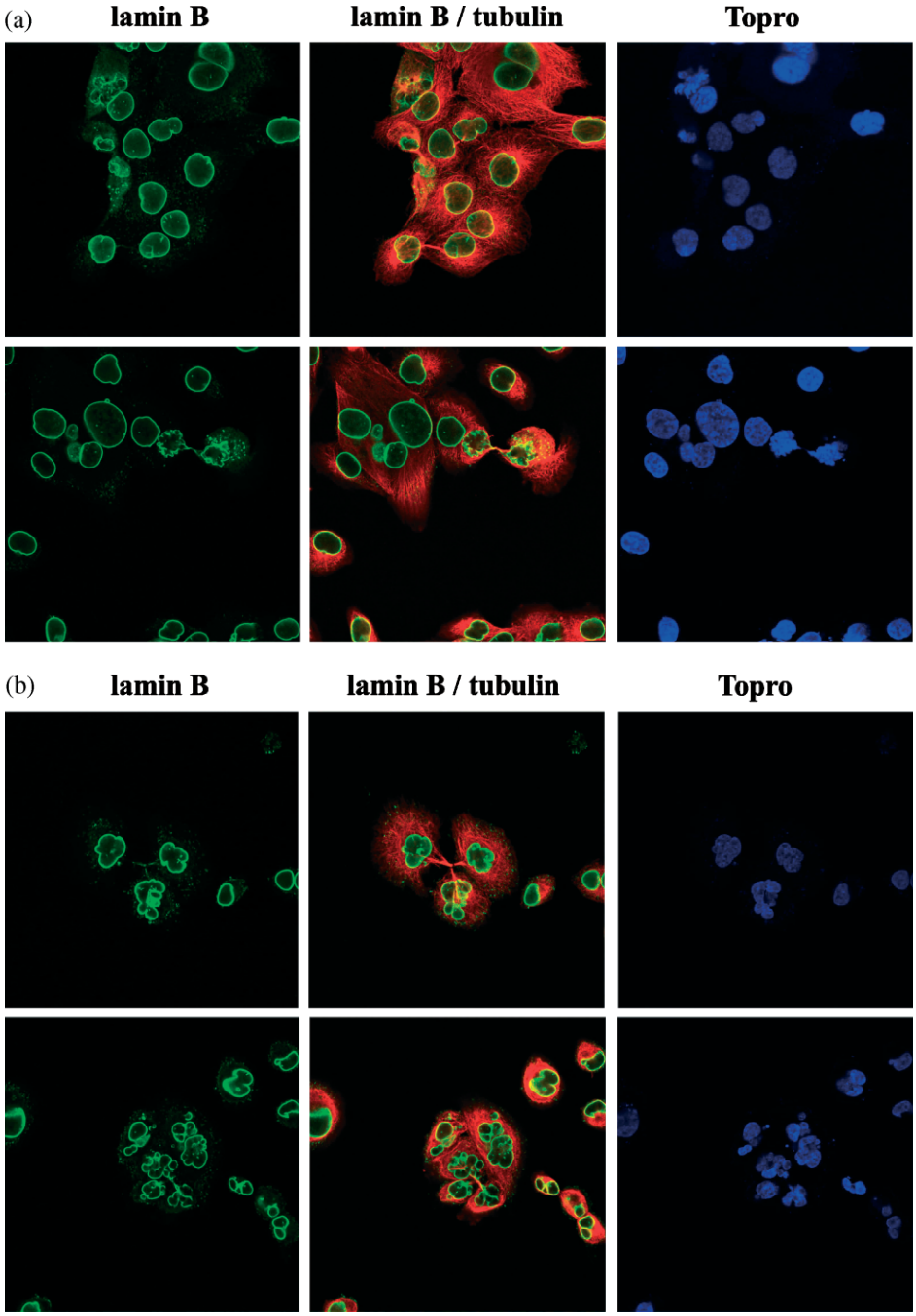

Figure 6 Representative images of DU cells treated with paclitaxel (A) and Ac-[Lys-Aib-Cys(CH_2CO-2′-Pac)]$_4$-NH_2 (tetra) (B). Cells that have been incubated with 3 nM of either drug for 24 h were cultured in a drug-free medium for 72 h and then immunostained for nuclear envelope (lamin B, green) microtubules (tubulin, red), and DNA (Topro, blue). Note the incorrect localization of lamin B during cytokinesis in the lower row of panel A and the abnormal cytokinesis (triple) in the upper row of panel B.

REFERENCES

1. Wani MC, Taylor HL, Wall ME, Coggon P, McPhail AT. Plant antitumor agents. VI. Isolation and structure of taxol, a novel antileukemic and antitumor agent from *Taxus brevifolia*. *J. Am. Chem. Soc.* 1971; **93**: 2325–2327.
2. Rowinsky EK, Donehower RC. Paclitaxel (taxol). *N. Engl. J. Med.* 1995; **332**: 1004–1014.
3. Blagosklonny MV, Fojo T. Molecular effects of paclitaxel: myths and reality (a critical review). *Int. J. Cancer* 1999; **83**: 151–156.
4. Theodoropoulos PA, Polioudaki H, Kostaki O, Derdas SP, Georgoulias V, Dargemont C, Georgatos SD. Taxol affects nuclear lamina and pore complex organization and inhibits import of karyophilic proteins into the cell nucleus. *Cancer Res.* 1999; **59**: 4625–4633.
5. Nicolaou KC, Riemer C, Kerr MA, Rideout D, Wrasidlo W. Design, synthesis and biological activity of protaxols. *Nature* 1993; **364**: 464–466.
6. Nuijen B, Bouma M, Schellens JHM, Beijnen JH. Progress in the development of alternative pharmaceutical formulations of taxanes. *Invest. New Drugs* 2001; **19**: 143–153.

7. Gelderblom H, Verweij J, Nooter K, Sparreboom V. Cremophor EL. the drawbacks and advantages of vehicle selection for drug formulation. *Eur. J. Cancer* 2001; **37**: 1590–1598.
8. Nicolaou KC, Yang Z, Liu JJ, Ueno H, Nantermet PG, Guy RK, Claiborne CF, Renaud JB, Couladouros EA, Paulvannan K, Sorensen EJ. Total synthesis of taxol. *Nature* 1994; **367**: 630–634.
9. Denis JN, Correa A, Greene AE. An improved synthesis of the taxol side chain and of RP 56976. *J. Org. Chem.* 1990; **55**: 1957–1959.
10. Danishefsky SJ, Masters JJ, Young WB, Link JT, Snyder LB, Magee TV, Jung DK, Isaacs RCA, Bornmann WG, Alaimo CA, Coburn CA, Di Grandi MJ. Total synthesis of baccatin III and taxol. *J. Am. Chem. Soc.* 1996; **118**: 2843–2859.
11. Kingston DGI, Chaudhary AG, Gunatilaka AAL, Middleton ML. Synthesis of taxol from baccatin III via an oxazoline intermediate. *Tetrahedron Lett.* 1994; **35**: 4483–4484.
12. Ojima I, Habus I, Zhao M. Efficient and practical asymmetric synthesis of the taxol C-13 side chain, N-benzoyl-(2R,3S)-3-phenylisoserine, and its analogs via chiral 3-hydroxy-4-aryl-beta-lactams through chiral ester enolate-imine cyclocondensation. *J. Org. Chem.* 1991; **56**: 1681–1683.
13. Brown S, Jordan AM, Lawrence NJ, Pritchard RG, McGown AT. A convenient synthesis of the paclitaxel side-chain *via* a diastereoselective Staudinger reaction. *Tetrahedron Lett.* 1998; **39**: 3559–3562.
14. Lee JW, Fuchs PL. Reduction of azides to primary amines in substrates bearing labile ester functionality. Synthesis of a PEG-solubilized, "Y"-shaped iminodiacetic acid reagent for preparation of folate-tethered drugs. *Org. Lett.* 1999; **1**: 179–182.
15. Ueda Y, Wong H, Matiskella JD, Mikkikineni AB, Farina V, Fairchild C, Rose WC, Mamber SW, Long BH, Kerns EH, Casazza AM, Vyas DM. Synthesis and antitumor evaluation of 2′-oxycarbonylpaclitaxels (paclitaxel-2′-carbonates). *Bioorg. Med. Chem. Lett.* 1994; **4**: 1861–1864.
16. Niethammer A, Gaedicke G, Lode HN, Wrasidlo W. Synthesis and preclinical characterization of a paclitaxel prodrug with improved antitumor activity and water solubility. *Bioconjugate Chem.* 2001; **12**: 414–420.
17. Lee JW, Lu JY, Low PS, Fuchs PL. Synthesis and evaluation of taxol – folic acid conjugates as targeted antineoplastics. *Bioorg. Med. Chem.* 2002; **10**: 2397–2414.
18. Deutsch HM, Glinski JA, Hernandez M, Haugwitz RD, Narayanan VL, Suffness M, Zalkow LH. Synthesis of congeners and prodrugs. 3. Water-soluble prodrugs of taxol with potent antitumor activity. *J. Med. Chem.* 1989; **32**: 788–792.
19. Kirschberg TA, VanDeusen CL, Rothbard JB, Yang M, Wender PA. Arginine-based molecular transporters: the synthesis and chemical evaluation of releasable taxol-transporter conjugates. *Org. Lett.* 2003; **5**: 3459–3462.
20. Lee JW, Lu JY, Low PS, Fuchs PL. Synthesis and evaluation of taxol-folic acid conjugates as targeted antineoplastics. *Bioorg. Med. Chem.* 2002; **10**: 2397–2414.
21. Chen X, Plasencia C, Hou Y, Neamati N. Synthesis and biological evaluation of dimeric RGD peptide-paclitaxel conjugate as a model for integrin-targeted drug delivery. *J. Med. Chem.* 2005; **48**: 1098–1106.
22. Wang S, Zhelev NZ, Duff S, Fischer PM. Synthesis and biological activity of conjugates between paclitaxel and the cell delivery vector penetratin. *Bioorg. Med. Chem. Lett.* 2006; **16**: 2628–2631.
23. Skwarczynski M, Hayashi Y, Kiso Y. Paclitaxel prodrugs: toward smarter delivery of anticancer agents. *J. Med. Chem.* 2006; **49**: 7253–7269.
24. Toniolo C, Crisma M, Formaggio F, Peggio C. Control of peptide conformation by the thorpe-ingold effect (C^{α}-tetrasubstitution). *Biopolymers (Pept. Sci.)* 2001; **60**: 396–419.
25. Tsikaris V, Sakarellos C, Sakarellos-Daitsiotis M, Orlewski P, Marraud M, Cung MT, Vatzaki E, Tzartos S. Construction and application of a new class of sequential oligopeptide carriers (SOC_n) for multiple anchoring of antigenic peptides: application to the acetylcholine receptor (AChR) main immunogenic region. *Int. J. Biol. Macromol.* 1996; **19**: 195–205.
26. Tsikaris V, Sakarellos C, Cung MT, Marraud M, Sakarellos-Daitsiotis M. Concept and design of a new class of sequential oligopeptide carriers (SOC) for covalent attachment of multiple antigenic peptides. *Biopolymers* 1996; **38**: 291–293.
27. Papas S, Strongylis C, Tsikaris V. Synthetic approaches for total chemical synthesis of proteins and protein-like macromolecules of branched architecture. *Curr. Org. Chem.* 2006; **10**: 1727–1744.
28. Jones J. Abbreviations and symbols in peptide science: a revised guide and commentary. *J. Pept. Sci.* 2006; **12**: 1–12.
29. Stewart JM, Young JD. *Solid Phase Peptide Synthesis.* 2nd edn. Pierce Chemical Company: Illinois, 1984; 43.
30. Stathopoulos P, Papas S, Tsikaris V. C-terminal N-alkylated peptide amides resulting from the linker decomposition of the Rink amide resin: a new cleavage mixture prevents their formation. *J. Pept. Sci.* 2006; **12**: 227–232.
31. Poon GK, Wade J, Bloomer J, Clarke SE, Maltas J. Rapid screening of taxol metabolites in human microsomes by liquid chromatography/electrospay ionization-mass spectrometry. *Rapid Commun. Mass Spectrom.* 1996; **10**: 1165–1168.
32. Jordan MA, Wendell K, Gardiner S, Derry WB, Copp H, Wilson L. Mitotic block induced in HeLa cells by low concentrations of paclitaxel (taxol) results in abnormal mitotic exit and apoptotic cell death. *Cancer Res.* 1996; **56**: 816–825.
33. Michalakis J, Georgatos SD, Romanos J, Koutala H, Georgoulias V, Tsiftsis D, Theodoropoulos PA. Micromolar taxol, with or without hyperthermia, induces mitotic catastrophe and cell necrosis in HeLa cells. *Cancer Chemother. Pharmacol.* 2005; **56**: 615–622.